Adsorption of chromium (VI) from aqueous solutions by cellulose modified with β-CD and quaternary ammonium groups

Yanmei Zhou [a,*], Qiang Jin [a], Tianwei Zhu [a], Yoshifumi Akama [b]

[a] *Institute of Environmental and Analytical Sciences, College of Chemistry and Chemical Engineering, Henan University, Jinming Street, Kaifeng, Henan 475004, PR China*
[b] *Department of Chemistry, Faculty of Science and Engineering, Meisei University, Hino, 191-8506 Tokyo, Japan*

ABSTRACT

Cellulose powder was grafted with the vinyl monomer glycidyl methacrylate using ceric ammonium nitrate as initiator and was further derived with β-CD and quaternary ammonium groups to build Cell-g-GMA-β-CDN$^+$ adsorbent. Epoxy cellulose was made up of Cell-g-GMA and Cell-hydro-g-GMA, and was found to contain 3.71 mmol g^{-1} epoxy groups. The adsorption process of the modified cellulose was described by the Langmuir model of adsorption well, and the maximum adsorption capacity of chromium (VI) reached 61.05 mg g^{-1}. The adsorption–desorption tests of β-CDN$^+$-type cellulose derivatives exhibited that the reproducibility of the adsorbent was well and the adsorbent could be reused five times at least.

© 2011 Elsevier B.V. All rights reserved.

1. Introduction

Although chromium (VI) compounds are extensively used in electroplating, anodizing operations in the surface finishing industry, corrosion control, oxidation, leather industry and various other industrial applications, they are known as a poisonous substance [1–4]. A long list of methods has been available for the removal of chromium (VI) such as chemical precipitation, ion exchanger, membrane separation, solvent extraction, and adsorption. Especially the adsorption is considered as one of the most popular techniques [5].

CDs are cyclic oligosaccharides built from six to eight (α = 6, β = 7, γ = 8) D-glucose units and are formed during the enzymatic degradation of starch and related compounds. CDs have gained prominence in recent years because of their cavity, which is hydrophobic in nature, capable of binding aromatic and other small organic molecules, and therefore provide ideal binding sites. CDs are widely used in basic research and industrial processes for the microencapsulation of unstable or volatile substance.

Recently, modified cellulose as a kind of cheaper and more effective sorbents has been investigated. Cellulose is not only renewable, biodegradable, and inexpensive, but also has many primary active hydroxyls which are easy to trigger many reactions, such as free radical reaction, esterification, halogenation, oxidation, and ether-

ification [6]. Various kinds of cellulose derivatives are synthesized by these reactions. Usually, a kind of modified cellulose is made up of carrier, grafting chain, and adsorption function groups. According to references [7,8], the effective adsorption function groups such as quaternary ammonium groups and ethylenediamine groups, were used for the treatment of chromium (VI) compounds from aqueous solutions.

In this study, chromium (VI) adsorption behavior on a novel modified cellulose containing β-cyclodextrin and quaternary ammonium groups as adsorption function groups in the aqueous solution was investigated (Scheme 1). The reproducibility of β-CDN$^+$ type modified cellulose derivatives was also studied. The new absorbent which contains β-cyclodextrin and quaternary ammonium groups, was expected to deal with the solution mixed of heavy metal ions and organic contaminants.

2. Experimental

2.1. Materials and reagents

Regenerated cellulose powder was used as the form of cellulose. Ceric ammonium nitrate (CAN), trimethylammonium (>33%), epichlorohydrin used in the tests were purchased from Sinopharm Chemical Reagent Co., Ltd. Glycidyl methacrylate (>99%, GMA) was obtained from Shangqiu Shengyuan Industrial Assistant Co., Ltd. and further treated by reduced pressure distillation method. β-Cyclodextrin (>98%, β-CD) was purchased from Shanghai Jianglai Biotechnology Co., Ltd. Potassium dichromate (K$_2$Cr$_2$O$_7$) was used

* Corresponding author. Tel.: +86 378 2868633x3422; fax: +86 378 3881589.
E-mail address: zhouyanmei@henu.edu.cn (Y. Zhou).
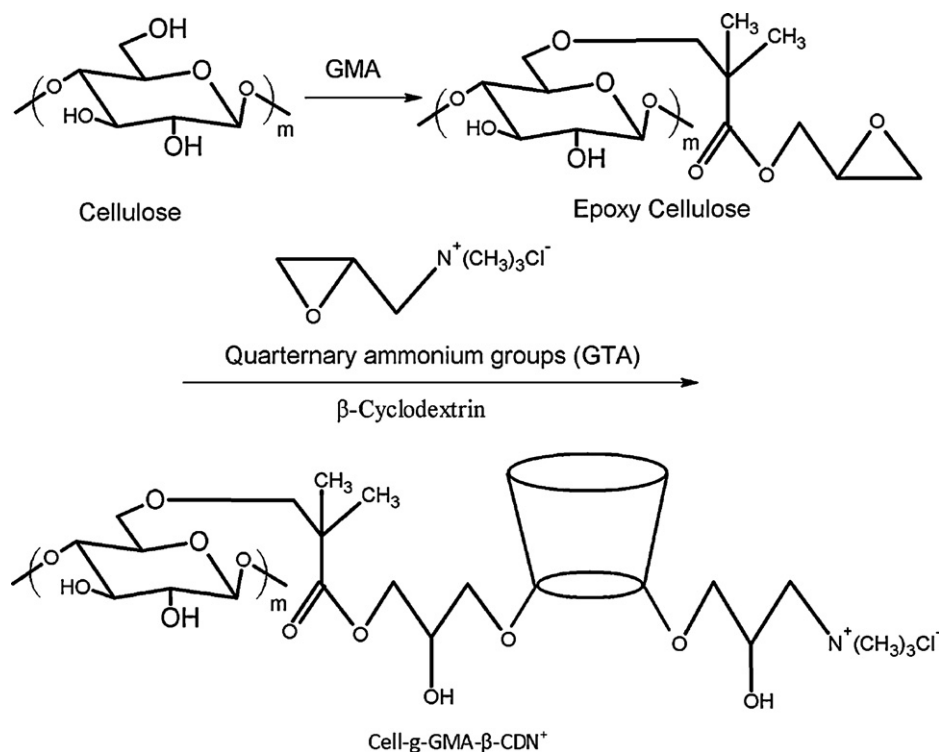
Scheme 1. Structure of β-CDN+ type chelating cellulose.

as a source of Cr (VI). All aqueous solutions and standards were prepared using deionized water.

2.2. Preparation of β-CDN+ type chelating cellulose

The poly(glycidyl methacrylate) [poly(GMA)] chains via polymerization of GMA were grafted on the surface of the cellulose using ceric ammonium nitrate as initiator [9]. In 500 mL round flask, cellulose (0.9 g) was initiated with CAN (0.12 mol) and 12 mL of 1 mol L^{-1} nitric acid in water (300 mL). The pH was adjusted to the range from 1.3 to 1.4 with nitric acid and sodium hydroxyl aqueous solution. Then, GMA (9 mL) was added to the flask, the contents of the flask were heated at 30 °C for 2.5 h under stirring in the N$_2$ atmosphere. The epoxy cellulose products were soxhlet extracted with acetone for 12 h to remove the GMA homopolymer, then dried at 60 °C under vacuum [10].

The quaternary ammonium groups were mainly made up of 2,3-epoxypropyltrimethylammonium chloride (GTA) and 3-chloro-2-hydroxypropyltrimethylammonium chloride (CTA) which was synthesized as reference [11] described. The intermediate product β-CDN+ was synthesized as the reference [12] described. The β-CD (13.75 g) was dissolved and stirred in NaOH solution for 24 h under room temperature. Then, quaternary ammonium group compounds (10.75 g) and H$_2$O (20 mL) were added. The reaction was carried out in water bath at 50 °C for 24 h. After the value of pH was adjusted to 7.0 with 5 mol L^{-1} nitric acid and sodium hydroxyl aqueous solution, epoxy cellulose (3.20 g) was added to the flask and dissolved in 150 mL DMF for 2 h. Then, NaCl (5.84 g) was added to the flask and the reaction was heated in water bath at 70 °C for 48 h [13,14]. The products were filtered off, washed with water, and then dried at room temperature under vacuum.

2.3. Determination of the content in adsorbent

2.3.1. Determination of the epoxy content of epoxy cellulose

The content of epoxy group in the epoxy cellulose was determined by the HCl–dioxane titration method. 0.15 mol L^{-1} HCl was reacted with the epoxy groups of epoxy cellulose in acetone solution. The residual HCl was back-titrated with 0.15 mol L^{-1} NaOH solution using phenolphthalein solution as indicator. The content of epoxy group in the epoxy cellulose Epv (mmol g^{-1}) was expressed as follows:

$$Epv = \frac{(V_0 - V_1)C_{NaOH}}{W_g} \tag{1}$$

where V_0 (mL) and V_1 (mL) are the titrimetric volume of NaOH by blank and sample consumed, respectively. C_{NaOH} (mol L^{-1}) is the amount of known NaOH molarity. W_g (g) is the weight of the epoxy cellulose.

2.3.2. Determination of the content of quaternary ammonium groups

The content of quaternary ammonium groups was determined by the sodium sulfite method [15]. Initially, CTA was reacted with sodium hydroxyl to transform into GTA using thymolphthalein solution as indicator. Then, GTA was able to react with sodium sulfite to open the active epoxy rings of GTA and sodium hydroxyl was produced which could be titrated by HCl. The content of quaternary ammonium groups could be calculated by the amount of HCl consumed.

2.3.3. Determination of the content of Cl$^-$ in adsorbent

The content of Cl$^-$ in adsorbent was determined by the AgNO$_3$ solution titration method [16]. This method is based on titration of the modified cellulose chloride salt with AgNO$_3$ in the aqueous solution.

2.4. Characterization of materials

2.4.1. FTIR characterization

The IR spectrum of the samples prepared by mixing 1 mg of each material with 100 mg of spectroscopy grade KBr was recorded from 4000 cm^{-1} to 400 cm^{-1} using a Thermo Nicolet Avatar 360 FTIR Spectrometer.

2.4.2. Scanning electron microscopy characterization

Scanning electron micrographs of samples were recorded using a Jeol JSM5600LV scanning electron microscope.

2.4.3. Elemental analysis characterization

The epoxy cellulose and Cell-g-GMA-β-CDN+ were dried previously and analyzed using a Perkin-Elmer 2400II equipment.

2.4.4. Thermogravimetric and differential thermal analysis

Thermogravimetric analysis (TGA) and the differential thermal analysis (DTA) were recorded using a Mettler-Toledo DTA/TGA instrument in the temperature range from 50 °C to 500 °C at a rate of 10 °C min^{-1} under nitrogen flow.

2.4.5. MAS NMR characterization

Cross polarization magic angle spinning (CPMAS) ^{13}C NMR spectra of Cell-g-GMA and Cell-g-GMA-β-CDN+ were recorded on a Bruker 400 (Avance III) spectrometer.

2.5. Batch adsorption studies

Batch adsorption studies were carried out by shaking 50 mg of Cell-g-GMA-β-CDN+ with 30 mL of the aqueous solution of chromium (VI) in different conical flasks using a temperature-controlled shaker for some time. Then, the mixtures were filtered out and the filtrate was analyzed for its chromium (VI) concentrations by 1,5-diphenylcarbohydrazide spectrophotometric method using a 7230G VIS recording spectrophotometer.

2.6. Desorption study

A glass column was used to pack 50 mg of adsorbent. A 50 mL sample solution containing appropriate amount of Cr (VI), after adjustment to pH 4.5, was passed through the column at a flow rate of 1.0 mL min^{-1}. After washings with distilled water, the adsorbed Cr (VI) was stripped from the adsorbent using a certain concentration of NaOH at a rate of 0.5 mL min^{-1}.

3. Results and discussion

3.1. Determination of the content in adsorbent

In this study, as shown in Eq. (1), the epoxy group content of the epoxy cellulose was calculated to contain 3.71 mmol g^{-1} by the HCl–dioxane titration method. The content of quaternary ammonium groups was calculated to contain 3.93 mmol g^{-1} by the sodium sulfite method. And the N+ content of adsorbent was determined by the AgNO$_3$ solution titration method. The Cl$^-$ content of adsorbent was calculated to contain 1.16 mmol g^{-1}.

3.2. Characterization of adsorbent

3.2.1. FTIR characterization

The FTIR spectra of the cellulose, epoxy cellulose, quaternary ammonium groups compound, and Cell-g-GMA-β-CDN+ are presented in Fig. 1. The spectrum of epoxy cellulose is featured by a strong band at 1729 cm^{-1} due to the absorption of carbonyl group,
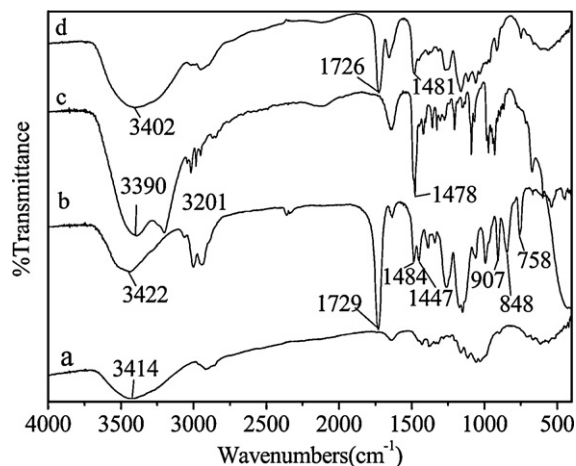

Fig. 1. FTIR of cellulose, epoxy cellulose, GTA/CTA mixture, and Cell-g-GMA-β-CDN+. (a) Cellulose; (b) Epoxy cellulose; (c) GTA/CTA mixture; (d) Cell-g-GMA-β-CDN+.

which can explain that the GMA has been grafted to the cellulose surface successfully [10]. A wide absorption peak at 3402 cm^{-1} is assigned to cellulose and β-CD OH groups while peaks at 2900 cm^{-1} is related to the C–H vibration of CH$_2$ groups. The peaks at 907, 848, and 758 cm^{-1} of epoxy cellulose were due to the absorption of epoxy groups. The peaks at 1481 cm^{-1} was due to C–N vibration of –N+(CH$_3$)$_3$Cl$^-$ and the peaks at 907, 848 758 cm^{-1} of epoxy groups disappeared, which indicated the epoxy groups of the epoxy cellulose were reacted with β-CDN+ group [17].

3.2.2. SEM characterization

Scanning electron micrographs presented in Fig. 2 show the surfaces of cellulose and Cell-g-GMA-β-CDN+.

The surface of the Cell-g-GMA-β-CDN+ is rougher than that of cellulose, which was due to the swelling effect of cellulose and the surface of cellulose grafted GMA and β-CDN+. The specific surface area of Cell-g-GMA-β-CDN+ became larger because of the heterogeneous surface. Obviously, the capability of Cr (VI)-removal by Cell-g-GMA-β-CDN+ will be much better.

3.2.3. Elemental analysis characterization

The percentage of carbon, hydrogen and nitrogen of epoxy cellulose and Cell-g-GMA-β-CDN+ was determined by elemental analysis method. The results are presented in Table 1. The percentage of nitrogen of Cell-g-GMA-β-CDN+ was 1.46%. The result indicated that epoxy cellulose was derived with β-CDN+ group effectively and in accord with the result by the AgNO$_3$ solution titration method.

3.2.4. TGA and DTA characterization

TGA and DTA curves of cellulose, epoxy cellulose, and Cell-g-GMA-β-CDN+ are presented in Figs. 3 and 4. The differences in thermal behavior of three samples lie in (1) the temperatures of initial weight loss, (2) the rate of weight loss, (3) the magnitude of the enthalpy change, and (4) the temperature corresponding to the values of the peak of the DTA curve [18]. The endothermic peak at 120 °C is due to evaporation of the water in the sample. The long

Table 1
Elemental analysis of epoxy cellulose and Cell-g-GMA-β-CDN+.

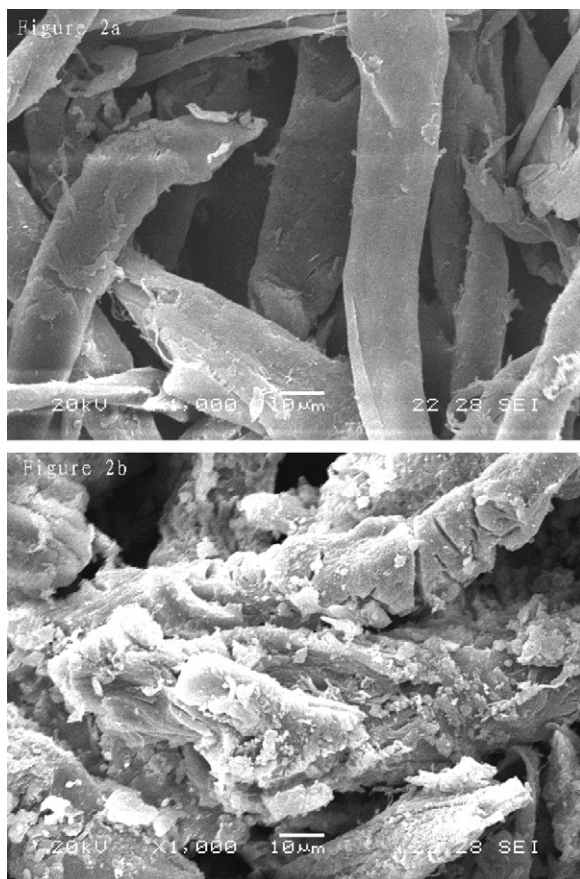| Type	C		H		N	
	%	mmol g^{-1}	%	mmol g^{-1}	%	mmol g^{-1}
Epoxy cellulose	51.45	42.8	6.72	66.5	–	–
Cell-g-GMA-β-CDN+	43.54	36.3	7.40	73.3	1.46	1.04

Fig. 2. SEM morphology of cellulose and Cell-g-GMA-β-CDN+. (a) Cellulose magnification 1000×; (b) Cell-g-GMA-β-CDN+ magnification 1000×.

endothermic process with a slow weight loss is due to dehydration and depolymerization-tar-forming processes in cellulose. The process from 240 °C to 370 °C is attributed to the thermal cleavage of the glycosyl units and scission of other C–O bonds via a free radical reaction [19]. In Fig. 4, there is an additional endothermic peak at 390 °C because of the degradation of poly(GMA) in the sample. The exothermic peak at 350 °C is due to some reactions of the epoxy group. The degradation of poly(GMA) occurs at 360 °C at first and completely at 435 °C [20]. The endothermic peak of DTA curve at 250 °C is due to the fusion of the Cell-g-GMA-β-CDN+ and epoxy groups grafted [21,22]. The units of D-glucose began to decompose into a lot of organic compounds in the temperature ranging
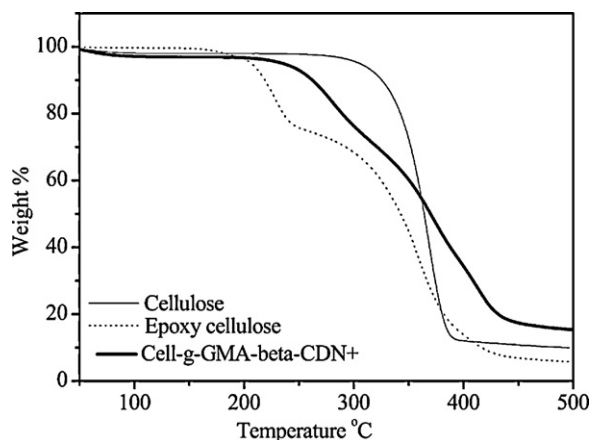

Fig. 3. TGA curves for cellulose, epoxy cellulose, and Cell-g-GMA-β-CDN+.

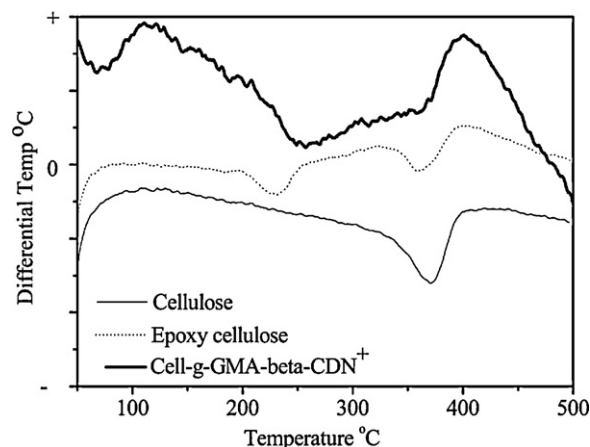**Fig. 4.** DTA curves for cellulose, epoxy cellulose, and Cell-g-GMA-β-CDN+.

from 300 °C to 450 °C [23]. The process from 250 °C to 425 °C can be interpreted as the decomposition of the new products with smaller chains because of the reaction of the water molecule in the tight crosslink of the polymer network [24].
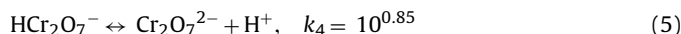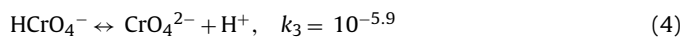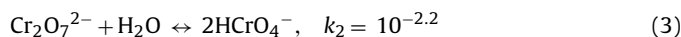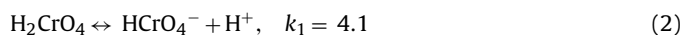
From the TGA curves, it can be seen that the thermal stability of epoxy cellulose becomes weaker, but the thermal stability of the epoxy group in the Cell-g-GMA-β-CDN+ is much better than that of epoxy cellulose.

3.2.5. MAS NMR characterization

The authentication of Cell-g-GMA-β-CDN+ by MAS ^{13}C NMR spectroscopy (Fig. 5b) confirms the occurrence of β-CDN+ reaction as well. In Fig. 5a, the signals from 1 to 6 are attributable to six carbon (C1–C6) atoms of the glucose unit of cellulose [25]. The signals 7 (δ: 16.8 ppm) and 9 (δ: 177.8 ppm) are attributable to C7 and carbon atoms of carbonyl C=O (C9), respectively. The signal 10 (δ: 49.5 ppm) is attributable to the carbon atoms (C10) of epoxy groups. In Fig. 5b, the signals from a to f are attributable to six carbon atoms of the glucose unit of cellulose and β-CD. As a result of the chemical environment of C10 (Fig. 5a) in epoxy groups changing, the shift of signal 10 changes 5.6 ppm. Thus, a new signal, signal j (δ: 55.1 ppm), appears in Fig. 5b. The signal k (δ: 57.8 ppm) is attributable to the carbon atoms of –CH2–N in β-CDN+.

3.3. Effect of pH on Cr (VI) adsorption

The removal of pollutants from wastewaters by adsorption is highly dependent on the pH of solution. The variation of pH can affect the surface charge of the adsorbent, the degree of ionization and speciation of adsorbate [26]. The equilibrium equations of chromium in solution are known as follows [27]:

$$H_2CrO_4 \leftrightarrow HCrO_4^- + H^+, \quad k_1 = 4.1 \tag{2}$$

$$Cr_2O_7^{2-} + H_2O \leftrightarrow 2HCrO_4^-, \quad k_2 = 10^{-2.2} \tag{3}$$

$$HCrO_4^- \leftrightarrow CrO_4^{2-} + H^+, \quad k_3 = 10^{-5.9} \tag{4}$$

$$HCr_2O_7^- \leftrightarrow Cr_2O_7^{2-} + H^+, \quad k_4 = 10^{0.85} \tag{5}$$

The plot of the percentage of Cr (VI) removed by Cell-g-GMA-β-CDN+ as a function of initial pH ranging from 2.0 to 8.0 is shown in Fig. 6. The optimum pH ranges from 4 to 6, while the adsorption rate of Cr (VI) decreases beyond the optimum pH range. This could be explained as follows: the equilibrium clearly reveals that at higher pH 7.8 the predominant form is CrO4²⁻ while between pH 2.0 and 6.0, HCrO4⁻ and Cr2O7²⁻ are in equilibrium. The quaternary ammonium groups of Cell-g-GMA-β-CDN+ have been protonated to
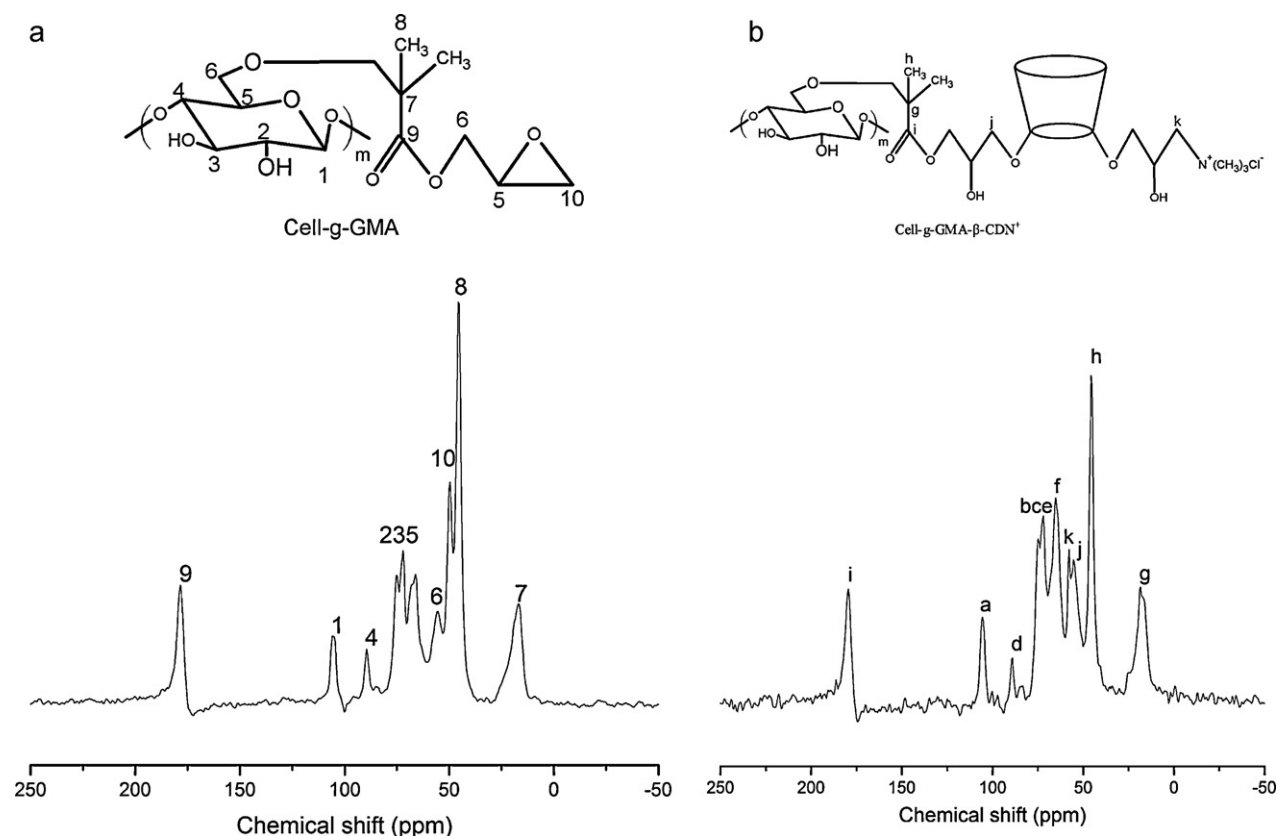
Fig. 5. MAS ^{13}C NMR spectra of Cell-g-GMA and Cell-g-GMA-β-CDN$^+$. (a) Cell-g-GMA; (b) Cell-g-GMA-β-CDN$^+$.

N$^+$(CH$_3$)$_3$ groups, which primarily act as an active site to form Cell-g-GMA-β-CDN$^+$–Cr complex compound. The HCrO$_4$$^-$ and Cr$_2$O$_7$$^{2-}$ with negative charge reacted with Cell-g-GMA-β-CDN$^+$ and Cell-g-GMA-β-CDN$^+$–Cr complex compound was obtained in aqueous solution during the pH range from 3 to 6. At the high initial pH, adsorption was reduced because the competitive adsorption of hydroxyl reacted with the chromium (VI). While, the competitive adsorption of Cl$^-$ reacted with the chromium (VI) at the low initial pH will reduce the percentage of Cr (VI) removal. So, the optimum initial pH was determined to be 4.5.

3.4. Effect of amount on Cr (VI) adsorption

The percentage of Cr (VI)-removal was studied by changing the amount of adsorbent from 10 to 65 mg while the concentration of chromium (VI) was 50 mg L^{-1} without change (Fig. 9). The total-chromium-removal efficiency increases with the amount of adsorbent up to an optimum dosage, beyond which the value of efficiency does not significantly change. This could be explained as follows: although increasing adsorbent dosage will provide larger surface area (or more adsorption sites), the concentration of initial Cr (VI) was fixed and the adsorbent was excessive when the amount of adsorbent overran the optimum dosage. As shown in Fig. 8, the optimum dosage was determined to be 50 mg.

3.5. Effect of diverse ions on Cr (VI) adsorption

There are various kinds of ions in wastewater. So, the effects of diverse ions of Cd^{2+}, F$^-$, H$_2$PO$_4$$^-$, Ca^{2+}, Co^{2+}, NH$_4$$^+$, Zn^{2+}, Mg^{2+}, Mn^{2+}, SO$_4$$^{2-}$ to Cr (VI) adsorbed in the batch method were also studied. The experimental results are shown in Table 2. It can been seen that 25 mL 50 mg L^{-1} of Cr (VI) in the solution were still adsorbed

effectively by Cell-g-GMA-β-CDN$^+$-type adsorbent when the solution contained other ions at the same time. In other words, the adsorbent could selectively adsorb Cr (VI) from the mixed solution effectively.

3.6. Kinetics study

Two important physical–chemical aspects of the process, the kinetics and the equilibrium of adsorption were used to evaluate the process of adsorption. Two rate equations were used to analyze the adsorption kinetics, data-pseudo-first-order kinetics and pseudo-second-order reaction kinetics [28]. The results are presented in Fig. 8 and Table 3.

Table 2
The effect of diverse ions.

Diverse ions	Concentration (mg L^{-1})		Adsorption of Cr (VI) (%)
	Diverse ions	Cr (VI) found	
Cd^{2+}	100	0.86	98.3
F$^-$	100	0.93	98.1
H$_2$PO$_4$$^-$	200	1.09	97.8
Ca^{2+}	200	2.38	95.2
Co^{2+}	100	1.49	97.0
NH$_4$$^+$	100	1.71	96.6
Zn^{2+}	100	1.05	97.9
Mg^{2+}	100	2.19	95.6
Mn^{2+}	50	3.36	93.3
SO$_4$$^{2-}$	10	1.34	97.3

Conditions: temperature, 18 °C; shaking time, 100 min; adsorbent, 50 mg; initial pH, 4.5; Cr (VI), 25 mL 50 mg L^{-1}.
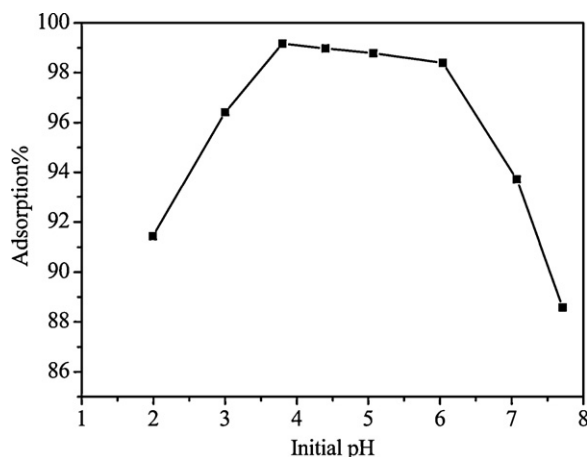
Fig. 6. Effect of pH on Cr (VI) adsorption. Conditions: 50 mg L^{-1} Cr (VI) solution; temperature, 18 °C; shaking time, 100 min; adsorbent, 50 mg.

Fig. 7. Effect of shaking time on Cr (VI) adsorption. Conditions: 50 mg L^{-1} Cr (VI) solution; temperature, 18 °C; initial pH, 4.5.

Lagergren's pseudo-first-order kinetics (Eq. (6)) can be represented in non-linearized form Eq. (7) and linear form Eq. (8).

$$\frac{dq_t}{dt} = k_1(q_e - q_t) \qquad (6)$$

$$q_t = q_e(1 - e^{-k_1 t}) \qquad (7)$$

$$\ln(q_e - q_t) = \ln q_e - k_1 t \qquad (8)$$

where k_1 is the pseudo-first-order rate constant of the adsorption process (g mg^{-1} min^{-1}). The values of q_e and k_1 are calculated by the non-linearized form Eq. (7), and the value of R^2 is carried out by the linearized form Eq. (8). The results are presented in Table 3.

Pseudo-second-order kinetics (Eq. (9)) can be used to assess the process of chromium (VI) absorbed concentration. Linearized form of pseudo-second-order kinetics is Eq. (10).

$$\frac{dq_t}{dt} = k_2(q_e - q_t)^2 \qquad (9)$$

$$\frac{t}{q_t} = \frac{1}{k_2 q_e^2} + \frac{1}{q_e} t \qquad (10)$$

where k_2 is the rate constant of the adsorption process (dm^3 mg^{-1} min^{-1}), q_e is the equilibrium amount of chromium (VI) adsorbed (mg g^{-1}), and q_t is the amount of chromium (VI) adsorbed at any time t (mg g^{-1}).

When $t \to 0$, the initial sorption rate, h can be defined as follows:

$$h = k_2 q_e^2 \qquad (11)$$

where q_e is the equilibrium sorption capacity, and k_2, the pseudo-second-order rate constant, can be determined experimentally from slope and intercept by plotting t/q_t against t.

We can obtain some results by analyzing Figs. 7 and 8 and parameters listed in Table 3. The kinetics of chromium (VI) adsorption on Cell-g-GMA-β-CDN$^+$ accords with the pseudo-second-order kinetic process correctly. Also, the plot showed an exact coefficient (R^2) which was coherent with the pseudo-second-order equation proposed.

Fig. 8. Pseudo-second-order sorption kinetics of Cr (VI) on Cell-g-GMA-β-CDN$^+$. Conditions: 50 mg L^{-1} Cr (VI) solution; temperature, 18 °C; adsorbent, 50 mg; initial pH, 4.5.

3.7. Adsorption isotherms

An adsorption isotherm can be used to characterize the interaction of metal ions with adsorbents. The isotherm provides a relationship between the concentration of metal ions in solution and the amount of metal ions adsorbed on the solid phase when both phases are in equilibrium [29]. The maximal adsorbance of adsorbent in different concentrations of Cr (VI) was examined and shown in Fig. 10. When the equilibrium concentration of Cr (VI) was changing in the range from 0 to 48.3 mg L^{-1}, the adsorption quantity of Cr (VI) was found to increase sharply. Then, the adsorption quantity of Cr (VI) did not significantly change. This is because the concentration of initial adsorbent was fixed and the adsorption sites were not enough for Cr (VI) when the concentration of Cr (VI) increased.

The equilibrium amount of Cr (VI) adsorbed per unit mass of adsorbent, q_e (mg g^{-1}) and its final concentration in solution,

Table 3
Pseudo-first-order and second-order-order models for adsorption of Cr (VI) onto Cell-g-GMA-β-CDN$^+$.

Kinetics models	Parameters				
	q_e (mg g^{-1})	k_1 (g mg^{-1} min^{-1})	k_2 (g mg^{-1} min^{-1})	h (mg g^{-1} min^{-1})	R^2
Pseudo-first-order	30.29	2.84×10^{-2}	–	–	0.0572
Pseudo-second-order	29.74	–	8.50×10^{-1}	751.88	0.9998

Conditions: concentration of Cr (VI) solution, 50 mg L^{-1}; temperature, 18 °C; adsorbent, 50 mg; initial pH, 4.5.
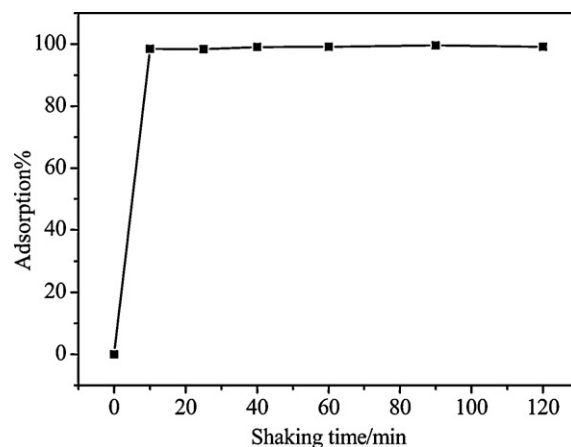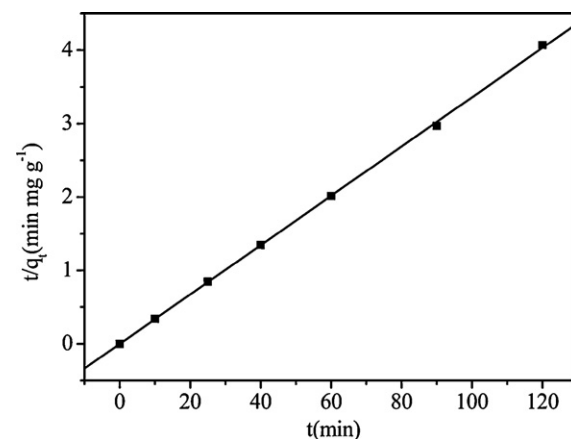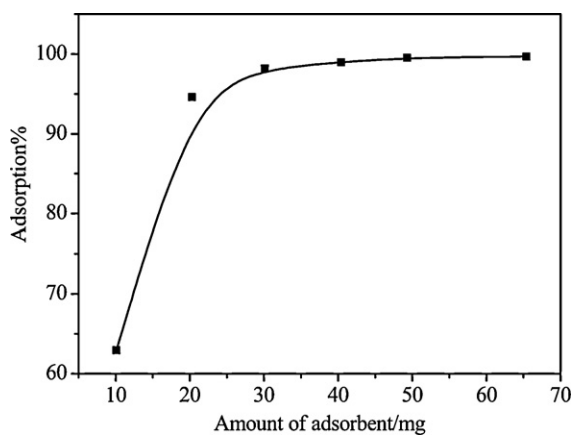
Fig. 9. Effect of amount of adsorbent on Cr (VI) adsorption. Conditions: 50 mg L^{-1} Cr (VI) solution; temperature, 18 °C; initial pH, 4.5; shaking time, 100 min.
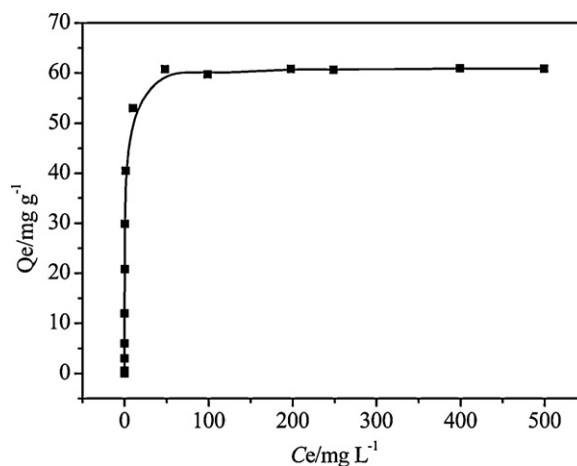

Fig. 10. Influence of Cr (VI) equilibrium concentration on the adsorption on Cr (VI).

C_e (mg L^{-1}) are related to adsorption isotherm. The adsorption isotherm models of Langmuir (Eq. (12)) and Freundlich (Eq. (14)), which are used to evaluate the adsorption experiments in function of the initial metal ion concentration in aqueous single solutions. The adsorption isotherm models of Langmuir and Freundlich can be represented in the linearized form of Eqs. (13) and (15), respectively.

$$q_e = \frac{Q^o b_L C_e}{1 + b_L C_e} \tag{12}$$

$$\frac{C_e}{q_e} = \frac{C_e}{Q^o} + \frac{1}{Q^o b_L} \tag{13}$$

$$q_e = K_F C_e^{1/n_F} \tag{14}$$

$$\ln q_e = \ln K_F + \frac{1}{n_F} \ln C_e \tag{15}$$

where Q^o, b_L are adsorption capacity and binding energy of adsorption of Langmuir, respectively. K_F and $1/n_F$ are adsorption capacity and the heterogeneity factor of Freundlich adsorption isotherm, respectively. q_e is the amount of solute adsorbed (mg g^{-1}), C_e is equilibrium concentration in solution (mg L^{-1}). Eq. (13) was used to determine the values of $1/Q^o b_L$ (intercept) and $1/Q^o$ (slope). Eq. (15) showed a logarithmic relationship between the adsorption quantity and equilibrium concentration. Fig. 11 is the Langmuir adsorption isotherm. And the parameters of isotherm models are presented in Table 4.

The values of Langmuir and Freundlich model correlation coefficient (R^2) were 0.9999 and 0.8352, respectively, which were calculated by Eqs. (13) and (15). Obviously, the adsorption process was described by the Langmuir isotherm model more correctly. The constants of Langmuir isotherm model were calculated by Eq. (13) and shown in Table 4. Q^o was calculated to be 61.05 mg g^{-1}.

3.8. Desorption

One of the important characteristics of chelating copolymers is their ability to be regenerated and reused.
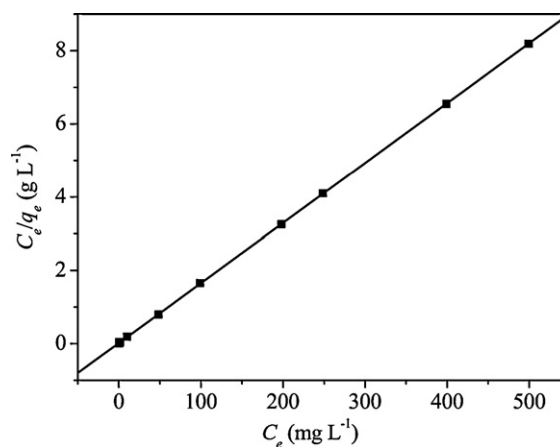

Fig. 11. Langmuir isotherm for Cr (VI) adsorption on Cell-g-GMA-β-CDN$^+$. Condition: temperature, 18 °C.

As shown in Fig. 6, the competitive adsorption of hydroxyl reacted with the chromium (VI) was more efficaciously under the alkaline condition. Thus, sodium hydroxide was predicted to be a desorption agent to obtain Cell-g-GMA-β-CDN$^+$-type adsorbent. The relationship between the desorption percentage and the concentration of sodium hydroxide was studied and shown in Fig. 12. And the optimum concentration of sodium hydroxide was determined to be 0.50 mg L^{-1}.

The adsorbent could be reused five times at least in the cycle of adsorption–desorption–adsorption, and the efficiency of Cr (VI) removed from solution almost did not change, which proved that the Cell-g-GMA-β-CDN$^+$-type adsorbent had excellent ability of reuse and regeneration.

Table 4
Langmuir and Freundlich isotherm models for adsorption of Cr (VI) onto Cell-g-GMA-β-CDN$^+$.

Isotherm models	Parameters				
	b_L (L mg^{-1})	K_F (L g^{-1})	Q^o (mg g^{-1})	n_F	R^2
Langmuir	0.9762	–	61.05	–	0.9999
Freundlich	–	13.9369	–	3.112	0.8352

Conditions: temperature, 18 °C; shaking time, 100 min; adsorbent, 50 mg; initial pH, 4.5.
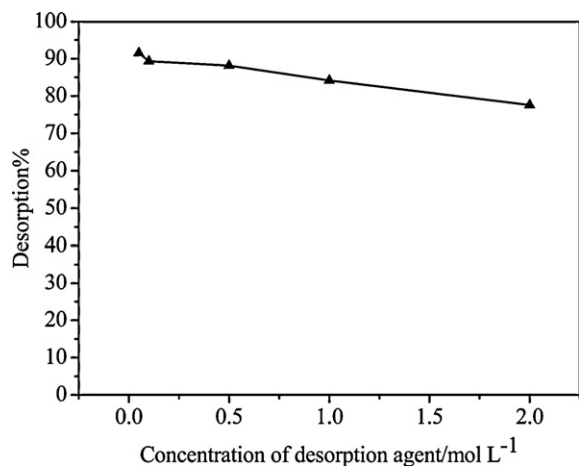
Fig. 12. Effect of concentration of desorption agent. Conditions: temperature, 18 °C; concentration of Cr (VI), 25 mL 500 mg L^{-1}; initial pH, 4.5; desorption agent, 50 mL NaOH.

4. Conclusions

A new type of adsorbent, Cell-g-GMA-β-CDN$^+$, was synthesized, characterized and applied to uptake chromium (VI) in water samples. Batch adsorption experiments were performed to evaluate the efficiency of Cell-g-GMA-β-CDN$^+$ towards Cr (VI) ions, and the effects of adsorption conditions on adsorptive performance were investigated. The adsorption process fit the assumptions of the Langmuir isotherm and the pseudo-second-order kinetics model, which was determined by the values of correlation coefficient (R^2). In the desorption experiments, the adsorbent could be reused five times at least with 0.5 mg L^{-1} sodium hydroxide as a desorption agent.

The Cell-g-GMA-β-CDN$^+$-type adsorbent has been proved as one of efficient adsorbents for the removal of toxic Cr (VI) from aqueous media. Also, the adsorbent will be used to adsorb heavy metal ions and organic pollutions because of the special characters of β-CD's cavity at the same time.

Acknowledgement

References

[1] P. Krauter, R. Martinelli, K. Williams, S. Martins, Removal of Cr (VI) from ground water by *Saccharomyces cerevisiae*, Biodegradation 7 (1996) 277–286.
[2] Z. Yang, B. Wang, L. Chai, Y. Wang, H. Wang, C.Q. Su, Removal of Cr (III) and Cr (VI) from aqueous solution by adsorption on sugarcane pulp residue, J. Cent. South Univ. Technol. 16 (2009) 101–107.
[3] N. Fiol, I. Villaescusa, M. Martínez, N. Miralles, J. Poch, J. Serarols, Biosorption of Cr (VI) using low cost sorbents, Environ. Chem. Lett. 1 (2003) 135–139.
[4] M. Tuzen, O.D. Uluozlu, M. Soylak, Cr (VI) and Cr (III) speciation on *Bacillus sphaericus* loaded diaion SP-850 resin, J. Hazard. Mater. 144 (2007) 549–555.
[5] G. Bayramoğlu, M.Y. Arica, Adsorption of Cr (VI) onto PEI immobilized acrylate-based magnetic beads: isotherms, kinetics and thermodynamics study, Chem. Eng. J. 139 (2008) 20–28.
[6] D.W. O'Connell, C. Birkinshaw, T.F. O'Dwyer, Heavy metal adsorbents prepared from the modification of cellulose: a review, Bioresour. Technol. 99 (2008) 6709–6724.
[7] G. Xing, S. Zhang, B. Ju, J. Yang, Study on adsorption behavior of crosslinked cationic starch maleate for chromium (VI), Carbohydr. Polym. 66 (2006) 246–251.
[8] G. Bayramoğlu, M.Y. Arica, Ethylenediamine grafted poly(glycidyl methacrylate-co-methylmethacrylate) adsorbent for removal of chromate anions, Sep. Purif. Technol. 45 (2005) 192–199.
[9] D.W. O'Connell, C. Birkinshaw, T.F. O'Dwyer, A modified cellulose adsorbent for the removal of nickel (II) from aqueous solutions, J. Chem. Technol. Biotechnol. 81 (2006) 1820–1828.
[10] R.R. Navarro, K. Sumi, M. Matsumura, Improved metal affinity of chelating adsorbents through graft polymerization, Water Res. 33 (1999) 2037–2044.
[11] N. Levy, N. Garti, S. Magdassi, Flocculation of bentonite suspensions with cationic guar, Colloid Surf. A 97 (1995) 91–99.
[12] E. Blomberg, A. Kumpulainen, C. David, C. Amiel, Polymer bilayer formation due to specific interactions between β-cyclodextrin and adamantane: a surface force study, Langmuir 20 (2004) 10449–10454.
[13] X. Zhao, B. He, Synthesis and characterization of polymer-immobilized β-cyclodextrin with a inclusion recognition functionality, React. Funct. Polym. 24 (1994) 9–16.
[14] C.A.B. Nava-Ortiz, G. Burillo, E. Bucio, C. Alvarez-Lorenzo, Modification of polyethylene films by radiation grafting of glycidyl methacrylate and immobilization of β-cyclodextrin, Radiat. Phys. Chem. 78 (2009) 19–24.
[15] Aromatics-determination of carbonyl compounds content-neutral sodium sulfite method, National standards of PR China (GB/T 14454.13-2008).
[16] Standard examination methods for drinking water-nonmetal parameters, National standards of PR China (GB/T 5750.5-2006).
[17] S.M. Gawish, S.R. Matthews, D.M. Wafa, F. Breidt, M.A. Bourham, Atmospheric plasma-aided biocidal finishes for nonwoven polypropylene fabrics. I. Synthesis and characterization, J. Appl. Polym. Sci. 103 (2007) 1900–1910.
[18] P. Yang, S. Kokot, Thermal analysis of different cellulosic fabrics, J. Appl. Polym. Sci. 67 (1996) 1137–1146.
[19] M. Huang, X. Li, Thermal degradation of cellulose and cellulose esters, J. Appl. Polym. Sci. 68 (1998) 293–304.
[20] S.R. Shukla, A.R. Athalye, Mechanical and thermal properties of glycidyl methacrylate grafted cotton cellulose, J. Appl. Polym. Sci. 57 (1995) 983–988.
[21] A. Raemy, T.F. Schweizer, Thermal behaviour of carbohydrates studied by heat flow calorimetry, J. Therm. Anal. Calorim. 28 (1983) 95–108.
[22] H. Li, L. Wang, K. Jacob, C.P. Wong, Syntheses, Characterizations of thermally degradable epoxy resins III, J. Polym. Sci. Polym. Chem. 40 (2002) 1796–1807.
[23] R.J. Evans, D.N. Wang, F.A. Agblevor, H.L. Chum, S.D. Baldwin, Mass spectrometric studies of the thermal decomposition of carbohydrates using ^{13}C-labeled cellulose and glucose, Carbohydr. Res. 281 (1996) 219–235.
[24] P.F. Britt, A.C. Buchanan, C.V. Owens Jr., J.T. Skeen, Does glucose enhance the 6 formation of nitrogen containing polycyclic aromatic compounds and polycyclic 7 aromatic hydro-carbons in the pyrolysis of proline? Fuel 83 (2004) 1417–1432.
[25] B. Belhalfaoui, A. Aziz, E.H. Elandaloussi, M.S. Ouali, L.C.D. Ménorval, Succinate-bonded cellulose: a regenerable and powerful sorbent for cadmium-removal from spiked high-hardness groundwater, J. Hazard. Mater. 169 (2009) 831–837.
[26] H.A. Elliott, C.P. Huang, Adsorption characteristics of some Cu (II) complexes on alumino-silicates, Water Res. 15 (1981) 849–855.
[27] J. Bajpai, R. Shrivastava, A.K. Bajpai, Dynamic and equilibrium studies on adsorption of Cr (VI) ions onto binary bio-polymeric beads of cross linked alginate and gelatin, Colloid Surf. A 236 (2004) 81–90.
[28] D.W. O'Connell, C. Birkinshaw, T.F. O'Dwyer, A chelating cellulose adsorbent for the removal of Cu (II) from aqueous solutions, J. Appl. Polym. Sci. 99 (2006) 2888–2897.
[29] A. Kara, L. Uzun, N. Beşirli, A. Denizli, Poly(ethylene glycol dimethacrylate-n-vinyl imidazole) beads for heavy metal removal, J. Hazard. Mater. 106 (2004) 93–99.